Development of an OSI SAF radiometer wind product

All radiometer wind products in the range
OSI-130 to OSI-132

Version: 1.0

Date: 19/08/2025

Sisma Samuel, Anton Verhoef and Ad Stoffelen

Royal Netherlands
Meteorological Institute
*Ministry of Infrastructure
and Water Management*

Document Change record

Document version	Software version	Date	Author	Change description
1.0		Aug 2025	SS	Initial version

Table of contents

1. Introduction

The Satellite Application Facilities (SAFs) are dedicated centres of excellence for processing satellite data – hosted by a National Meteorological Service – which utilise specialist expertise from institutes based in Member States. EUMETSAT created SAFs to complement its Central Facilities capability in Darmstadt. The Ocean and Sea Ice Satellite Application Facility (OSI SAF, http://osi-saf.eumetsat.int/) is one of eight EUMETSAT SAFs, which provide users with operational data and software products. Information on all SAFs can be obtained at https://www.eumetsat.int.

KNMI is involved in the OSI SAF as a centre where level 2 ocean-surface vector wind processing is carried out and associated L1 processing and calibration is supported by KNMI for all producers. Most of the wind products are based on scatterometers, which provide high accuracy at both nominal winds and at extreme winds [1], [2]. With the launch of the Microwave Imager (MWI) onboard European Polar Satellites of the Second Generation (EPS-SG), radiometer wind speeds will be added to the portfolio. Users are generally interested in consistent ocean surface wind products, where radiometer winds will particularly profit from the excellent scatterometer (SCA) heritage. A growing virtual scatterometer constellation provides stable, independent and intercalibrated vector winds over the ocean and its compatibility with background-informed passive microwave wind speeds is investigated to prepare for the EPS-SG satellites that will carry both scatterometers and radiometers. The SCA will be intercalibrated with the virtual scatterometer constellation and is expected to represent a very stable and accurate reference, as an ASCAT follow-on [3], [4], with winds calibrated against global moored buoy winds over several decades [5]. Moreover, relative scatterometer calibration does not require dependency on a background profile [6]. In this report the results of the Special Sensor Microwave Imager/Sounder (SSMIS) 1D-Var processing are compared with a well collocated scatterometer to prepare for the synergistic processing of MWI and SCA onboard EPS-SG. Information about the specific wind products and their status can be found on https://scatterometer.knmi.nl/.

MWI is a conically scanning microwave radiometer that measures thermally emitted radiations by the earth in the microwave regime between 18-183 GHz. MWI provides measurements of cloud, precipitation, water vapour and temperature profiles. The lower frequency channels also provide all-weather surface information. In this report the development of an OSI SAF radiometer surface wind speed product is described.

For processing surface wind speed from MWI, OSI SAF will follow the methodology already used in the Climate Monitoring Satellite Application Facility (CMSAF) for creating the Hamburg Ocean Atmosphere Parameters and Fluxes from Satellite Data (HOAPS). The software packages such as 1D-Var and RTTOV from the Numerical Weather Prediction Satellite Application Facility (NWP SAF) will be used.

Following the introduction, Section 2 provides an overview of microwave imagers, describing their key components and functionality. Section 3 outlines the input data used for the wind retrieval process, including the pre-processing algorithm applied to prepare the data for analysis, optimization with scatterometer winds and its validation. Section 4 provides the spatial pattern of wind speed and the comparison of retrievals under all sky and clear sky conditions. Finally, Section 5 offers the conclusions, summarizing the findings and suggesting areas for future research.

2. Microwave Imager (MWI)

The EPS-SG Microwave Imager (MWI) is a conically scanning radiometer measuring the naturally emitted radiation by the Earth surface in the microwave regime (18–183 GHz). The conical scanning rotating antenna has a constant incidence angle of about 53° to receive maximum polarized signal. The observations are acquired within an azimuth angle range of ±65° in the fore view, resulting in a swath width of 1700 km. The scan geometry of MWI is shown in Figure 1.

The MWI has heritage from previous instruments such as the Special Sensor Microwave/Imager (SSM/I) on the Defence Meteorological Satellite Program, Special Sensor Microwave Imager Sounder (SSMIS), the Tropical Rainfall Measuring Mission (TRMM) Microwave Imager (TMI) and the Advanced Microwave Scanning Radiometer (AMSR-E).

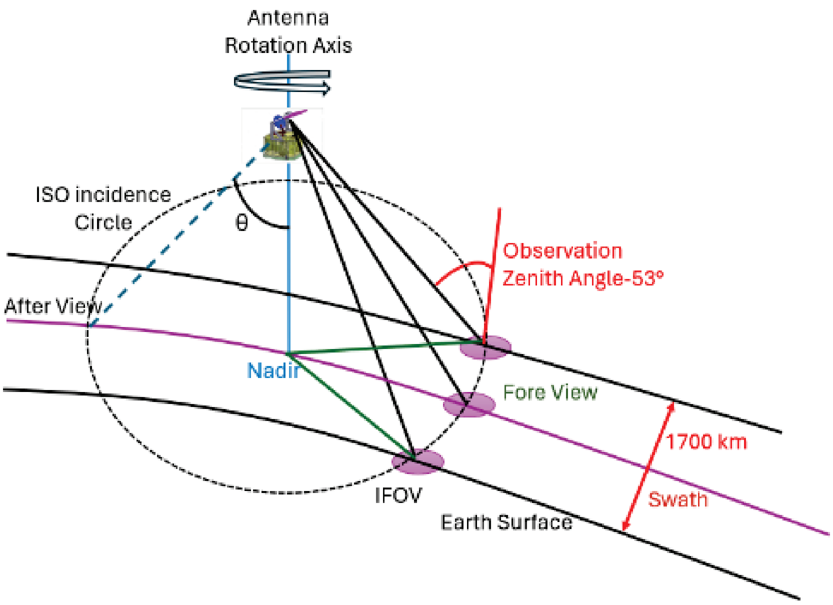

Figure 1: MWI Scan geometry.

MWI provides observations in 26 channels from 18 to 183 GHz with orthogonal horizontal (H) and vertical (V) polarizations for frequences up to 89 GHz. The low-frequency channels, 18.7 GHz (MWI-1) and 23.8 GHz (MWI-2), have an Integrated Field Of View (IFOV) of 59 km × 36 km, while the 31.4 GHz channel (MWI-3) has a resolution of 36 km × 22 km, and the 89 GHz channel has a resolution of 12 km × 7 km. The number of samples in one scan is 1,394 for all channels, with a sampling time of approximately 0.394 ms (2.60 km). The oversampling factor is about 20 for MWI-1 and MWI-2, about 10 for MWI-3, and 3–5 for MWI-8 [7]. The MWI mission enables the retrieval of various geophysical products, including precipitation over the ocean, total column water vapor, and cloud liquid water. Additionally, it provides all-weather surface imagery, such as sea ice coverage and type, snow coverage and water equivalent, and near-surface wind speed over the ocean, complementing scatterometer measurements.

3. Retrieval Method & Validation

3.1. 1D-VAR Retrieval Method

MWI wind retrieval is based on the algorithms developed for the HOAPS climate data record from SSMI/ and SSMIS [8]. In this work, we have used SSMIS data to develop and test our wind retrievals. The 1D-VAR approach is used for estimating near-surface wind speed from SSMIS observations and the retrievals are optimized using collocated and concurrent RapidScat measurements to prepare for the synergetic processing of MWI and SCA onboard EPS-SG. SSM/I sensors have been flown aboard the Defense Meteorological Satellite Program (DMSP) since 1987. For surface wind retrievals, the present study uses low frequencies such as 19.35, 22.235, 37.0, and 91.65 GHz as shown in Table 1. The 1D-VAR technique is based on Bayesian principles, and geophysical parameters are retrieved using the optimal estimation technique by Rodgers [9]. For the 1D-VAR technique, background (or prior) information of the atmosphere and surface states and the Brightness Temperature observations (T_B) are combined in an optimal way to statistically estimate the most probable state $\boldsymbol{x}$ of the atmosphere. The best estimate of $\boldsymbol{x}$ is estimated by minimizing the cost function $J(\boldsymbol{x})$.

$$J(\boldsymbol{x}) = \frac{1}{2}(\boldsymbol{x} - \boldsymbol{x_b})^T \boldsymbol{B}^{-1}(\boldsymbol{x} - \boldsymbol{x_b}) + \frac{1}{2}\big(\boldsymbol{y} - \mathcal{H}(\boldsymbol{x})\big)^T \boldsymbol{R}^{-1}\big(\boldsymbol{y} - \mathcal{H}(\boldsymbol{x})\big) \qquad \text{Eq.(1)}$$

where $\boldsymbol{x}$ is the atmospheric state, $\boldsymbol{x_b}$ is the background profile, $\boldsymbol{y}$ is the observed brightness temperature, $\boldsymbol{B}$ is the background error covariance matrix, $\boldsymbol{R}$ is the observational error covariance matrix, and $\mathcal{H}(\boldsymbol{x})$ is the observation operator (here, a radiative transfer model).

To extract the necessary physical information from the input profile dataset, a forward model that maps the physical state into T_B is used. Radiative Transfer for TOVS (RTTOV) along with RTTOV-SCATT is used to describe the propagation of radiation through absorbing, emitting, and scattering media in the microwave regime under all-sky condition [10]. The ocean surface emissivity is estimated using the SURFEM (SURface Fast Emissivity Model) which provides better precision over cold sea surface temperatures and high wind speed, as compared to the previous FASTEM model [11]. RTTOV calculates T_B for the background atmospheric state and for all subsequent states $\boldsymbol{x}$.

Channel No	Frequency [GHz]	Bandwidth [MHz]	Polarisation	Pixel size [km]
12	19.35	355	H	25x12.5
13	19.35	356.7	V	25x12.5
14	22.235	407.4	V	25x12.5
15	37	1545	H	25x12.5
16	37	1615	V	25x12.5
17	91.65	1615	V	12.5x12.5
18	91.65	1615	H	12.5x12.5

Table 1: SSMIS channels for surface wind speed retrieval.

The minimum gradient found of $J(\boldsymbol{x})$ with respect to $\boldsymbol{x}$ for a given measurement $\boldsymbol{y}$ estimates the most probable solution for $\boldsymbol{x}$. The Marduardt-Levenberg non-linear least square-based local minimization algorithm is used to solve and minimize the cost function. In addition to the minimization criteria, a T_B filtering is applied such that the difference between observed T_B and initially simulated T_B is less than 20 K for each channel, thereby reducing larger mismatches in retrievals. If this criterium is not met, no retrieval will be attempted. An overall bias correction was further applied to the brightness temperatures in the wind processing software for each channel. After bias correction, the best profile is estimated by minimizing a cost function, penalizing differences between simulated and observed brightness temperatures. After the wind retrieval, the 1D-VAR cost function value of the estimated solution, the retrieval residual, is evaluated. If its value is above a certain threshold (8.0), the retrieved wind is flagged as invalid.

3.2. Determination of background profiles for retrieval

The retrieval process requires a background profile as first guess of the atmospheric state. For the present study, the background profile used as a first guess of the atmospheric state may come from ERA5 forecast data or from a database of NWP SAF model profile data at 137 pressure levels. These background profiles are reduced to 43 pressure levels using interpolation with respect to the natural logarithm of the model level pressure. The background profile includes atmospheric temperature, humidity and cloud liquid water content (CLWC) at 43 levels and surface parameters such as the u and v components of surface wind, sea surface temperature and mean sea level pressure.

For the retrievals, the background profiles are initially taken from a NWP SAF model database [12], which consists of 25,000 profiles representing diverse humidity, precipitation, temperature, and cloud condensate conditions derived from global short-range forecasts [8]. These profiles extend vertically from the surface to 0.01 hPa. Around 13,000 profiles in the database are over the ocean and are used to construct an initial background state. The model profiles contain temperature, humidity and cloud liquid water in 137 model levels and surface parameters such as u and v surface wind vector components, mean sea level pressure, surface temperature etc. [12]. These model levels are reduced to 43 levels. Matching background profiles from the NWP SAF model dataset are selected based on thresholds for sea surface temperature (SST) and near-surface wind speed. Profiles are selected if the near-surface wind speed is within 2 m/s and the SST is within 2 K w.r.t the ERA5 forecast model values at the specific time and location of the satellite observation. For the selected profiles, the brightness temperatures are simulated using the forward model and a profile is computed using a weighted average. The weight of each contributing profile is computed using the variance of the differences $T_{B, \text{simulated}}$ - $T_{B, \text{observed}}$ of the channels A T_B filtering technique is applied such that the difference between simulated and observed T_B is less than 20 K for each channel, thereby reducing larger mismatches in retrievals. If this criterium is not met, no retrieval will be attempted. Alternatively, ERA5 forecast data are also used as initial background profiles for the retrievals. The datasets include hourly forecasts from +03 to +18 hours initiated at 06 and 18 UTC for model level temperature, specific humidity, cloud liquid water content and surface fields (u and v wind vector components, mean sea level pressure, surface temperature). The model data are quadratically interpolated with respect to time and bi-linearly interpolated with respect to location. SST is taken at analysis time (06 and 18 UTC). To identify the optimal combination of number of channels and background profile for wind retrieval experimental runs were conducted separately using (i) five channels (Channels 12–16) and (ii) seven channels (Channels 12–18) with two different background profiles with bias correction as discussed in Section 3.4. These experiments are verified with RapidScat.

Table 2 presents the average bias, SDD, and the number of collocations with RapidScat wind speed using both NWP SAF and ERA5 profiles for October 2014 [9]. Due to the large number of collocations with RapidScat, one month of data is sufficient to obtain reliable statistics. Similarly, the retrieved winds are compared to ECMWF model winds for 01-09 October 2014, as shown in Table 4. The SDD between the ERA5 background wind speed to RapidScat has an SDD of 1.32 m/s, whereas the retrieved SSMIS wind speed retrieved using ERA5 profiles has a lower SDD of 1.04 m/s. Similarly, the NWPSAF model profile wind speed has a SDD of 1.50 m/s when compared to RapidScat, while the SSMIS wind retrievals using NWPSAF profiles have a reduced SDD of 1.21 m/s. Recall that the wind speed background error variance for the retrievals in Table 2, Table 3, Table 4 and Table 5 is set to the square of the wind speed standard deviation of 1.4 m/s (the default value in NWPSAF-1DVar). Table 3 and Table 5 show the average bias and SDD for the common retrievals available in the preceding tables, respectively. The wind retrieval using seven channels with ERA5 forecast data as background profiles gives better results with the lowest bias and standard deviation with respect to RapidScat winds from all configurations. On the other hand, the number of retrieved winds is the lowest in this configuration, a more stringent quality control (QC) in other configurations leads to lower retrieved numbers and lower biases and standard deviations as well, as one might expect.

Table 3 indeed shows lower SDD against RapidScat for the common retrievals, effectively using both the QC associated with the NWP SAF profiles and the ERA5 profiles. These results demonstrate that using retrieved wind speeds with both NWP SAF model profile data and ERA5 is significantly improved when compared with independent RapidScat observations. Clearly, using ERA5 profiles and 7 channels provides the lowest SDD for this weather sample. Similarly, in a dependent validation, and Table 5 shows that ERA5 profiles are better suited to fit the SSMIS measurements than the NWP SAF profiles. However, using 5 or 7 channels provides a similar fit in terms of SDD, depending on weather sample (QC).

Background Profile	NWP SAF Profiles		ERA5 Profiles	
	5 channels	7 channels	5 channels	7 channels
Average Bias (ms^{-1})	0.35	0.59	0.25	0.17
SDD (ms^{-1})	1.21	1.21	1.12	1.04
No. of Collocations	1,101,347	1,101,347	1,066,774	1,001,391

Table 2 : Average SSMIS bias, SDD and no. of collocations with RapidScat wind speed using NWP SAF and ERA5 as background profiles during October 2014.

	No. of common collocation with RapidScat: 969,343			
Background Profile	NWP SAF Profiles		ERA5 Profiles	
	5 channels	7 channels	5 channels	7 channels
Average Bias (ms^{-1})	0.35	0.60	0.17	0.12
SDD (ms^{-1})	1.09	1.11	1.05	1.03

Table 3: Average SSMIS Bias, SDD and no. of common collocations with RapidScat using NWP SAF and ERA5 as background profiles during October 2014.

Background Profile	NWP SAF Profiles		ERA5 Profiles	
	5 channels	7 channels	5 channels	7 channels
Avg. Bias (ms^{-1})	0.49	0.67	0.26	0.18
SDD (ms^{-1})	0.98	1.08	0.83	0.77
No. of Collocations	8,962,653	9,094,677	8,683,227	8,150,464

Table 4: Average Bias, SDD and no. of collocations with ECMWF model wind speed using NWP SAF and ERA5 as background profiles on 01-09 October 2014.

	No. of common collocation with ECMWF: 8,078,071			
Background Profile	NWP SAF Profiles		ERA5 Profiles	
	5 channels	7 channels	5 channels	7 channels
Average Bias (ms^{-1})	0.46	0.65	0.18	0.13
SDD (ms^{-1})	0.95	1.02	0.73	0.76

Table 5: Average Bias, SDD and no. of common collocations with ECMWF model wind speed using NWP SAF and ERA5 as background profiles on 01- 09 October 2014.

3.3. Determination of R-matrix & B-matrix

The average standard deviation of the difference (SDD) of simulated and observed brightness temperature serves as the basis for the ***R***-matrix. Initially, for low-frequency channels (19.35, 22.235, and 37 GHz), the ***R***-matrix is set to twice the SDD, while for the high-frequency channel (91.65 GHz), it is four times the SDD to account for scattering effects. For the present study, the ***R***-matrix used for the retrievals follows the same approach as described in the SSMI/S validation report by HOAPS [8].

In the present study, the ***R*** matrix has only diagonal values representing the observation and forward model error. Higher ***R*** values correspond to lower weight in the cost function for the associated channel. Hence, the high R matrix values reduce the impact of each observation in the final result; this is done to prevent overfitting to the observations. Overfitting might occur due to oversampling or error correlation between observations [13]**.** The sensitivity of wind speed to T_B is estimated for seven channels as shown in Table 6. H-polarized channels exhibit greater sensitivity to wind speed compared to V-polarized channels. Similarly, horizontally polarized channels are more sensitive to surface roughness and foam compared to vertically polarized channels. Consequently, vertically polarized channels are assigned higher weight (lower ***R***-matrix values) as they are less influenced by surface roughness, while horizontally polarized channels have lower weight (higher ***R***-matrix) values [14]. The optimal values of ***R***-matrix are also validated using collocated and concurrent RapidScat measurements. The forward model RTTOV estimates the simulated T_B on top of the atmosphere. The background profile includes atmospheric temperature, humidity and cloud liquid water content at 43 levels and surface parameters such as u and v wind vector components, mean sea level pressure, surface temperature, and sea surface temperature. The associated uncertainty is represented by the background error (BE) covariance matrix (***B***-matrix), which consist of uncertainty associated with temperature at 43 atmospheric levels, the specific humidity in the lowest 26 levels, surface temperature, surface specific humidity, and skin temperature. In the 1D-

Var system, the background error covariance for wind speed, liquid water path, and surface emissivity is specified using constant values.

3.4. T_B Bias Correction

Figure 2 shows the scatter plot of simulated T_B and observed T_B for SSMIS before bias correction. The bias correction was further applied in the wind processing software for each channel. This empirical correction reduces the average bias between simulated and observed T_B for each channel as shown in Figure 3.

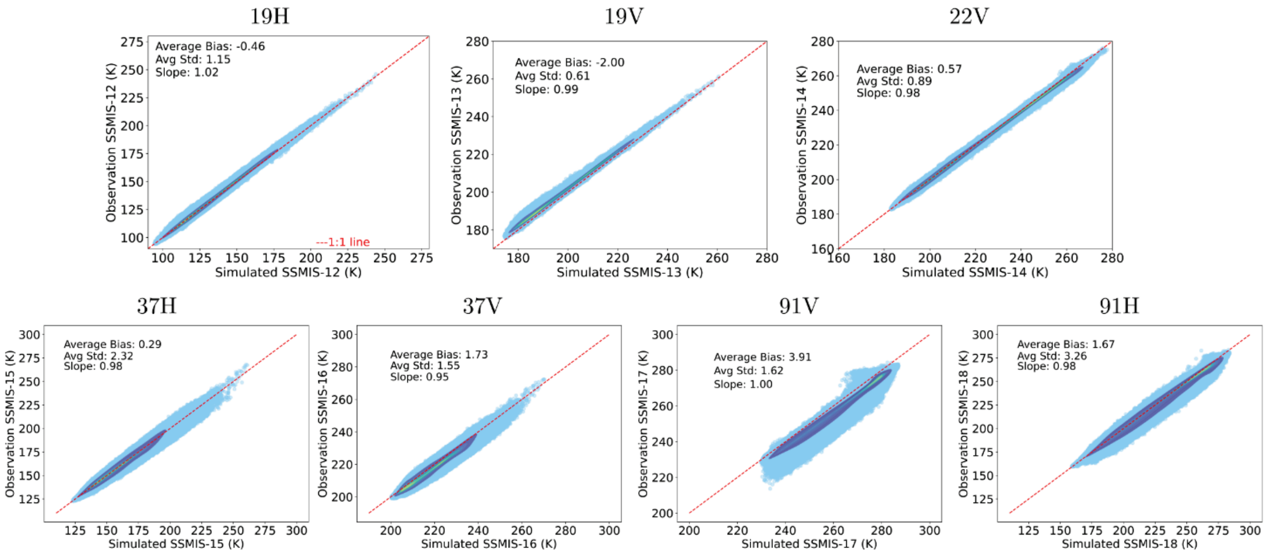

Figure 2: Scatter plot of Simulated TB and observed TB form SSMIS before bias correction using ERA5 background profiles during October 2014.

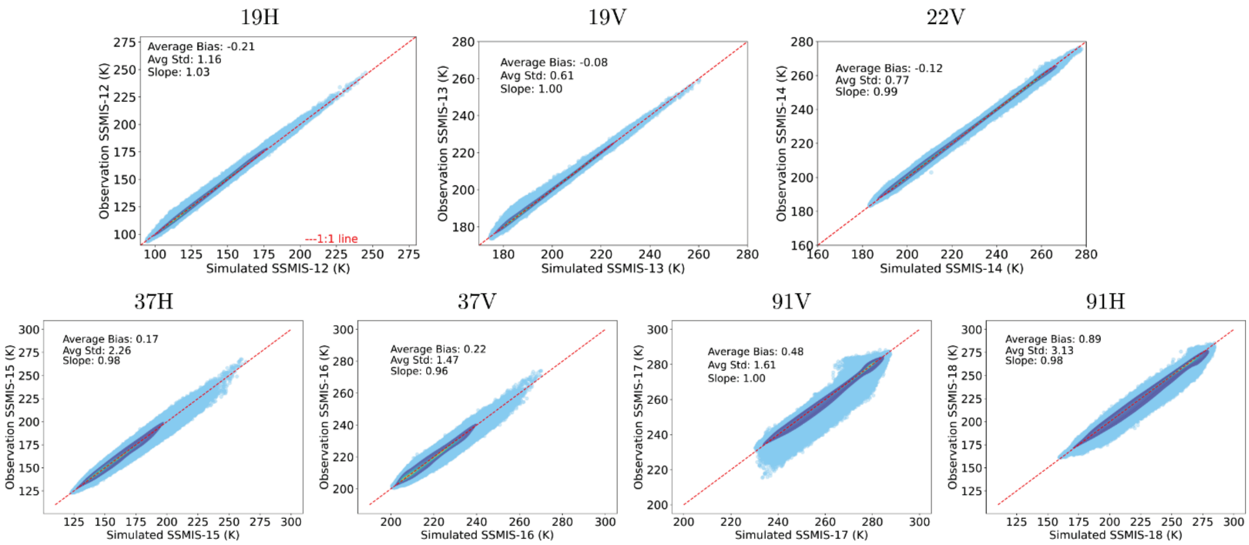

Figure 3: Scatter plot of Simulated TB and observed TB form SSMIS after bias correction using ERA5 background profiles during October 2014.

The average bias correction resulted in a 55-65% reduction in the cost function relative to the case without bias correction with values varying for each SSMIS orbit. After applying the bias correction, the average wind speed bias is reduced from 0.73 m/s and 0.76 m/s to 0.17 m/s when compared to both ERA5 winds and RapidScat winds. The wind speed SDD also decreases from 0.79 m/s to 0.76 m/s, and from 1.09 m/s to 1.04 m/s when compared to ERA5 and RapidScat winds, respectively. To evaluate seasonal variability in the average bias between simulated and observed T_B, retrievals were performed on ten representative days per season throughout 2014 without applying bias correction. The results indicate that the average biases remain stable throughout the seasons, with variations of less than 0.1K for each channel. The SDD between simulated and observed T_B showed minimal variation compared to the SDD obtained without bias correction, indicating that the retrieval remained stable under these adjustments. The minimal variation is attributed to the bias correction, which slightly alters the simulated brightness temperatures and consequently, the SDD, probably due to numerical effects.

Channel No	Average Bia s[K] (no bias correction)	SDD [K] (no bias correction)	Sensitivity [K/ms^{-1}]	R-matrix [K]	Average Bias [K] (after bias correction)	SDD [K] (after bias correction)
12 (19H)	-0.46	1.15	1.57	2.3	-0.21	1.16
13 (19V)	-2.0	0.61	0.5	1.22	-0.08	0.61
14 (22V)	0.57	0.89	0.6	1.78	-0.12	0.77
15 (37H)	0.28	2.32	1.6	4.62	0.17	2.26
16 (37V)	1.72	1.55	0.35	3.1	0.22	1.47
17 (91V)	3.91	1.62	0.32	6.44	0.48	1.61
18 (91H)	1.67	3.26	1.53	13.04	0.89	3.13

Table 6 : Average bias between simulated and observed TB for each SSMIS channel before and after bias correction, sensitivity of wind retrieval to TB, and observational error matrix (R-matrix) values for ERA5 background profiles.

3.5. Determination of Wind Speed BE variance

The uncertainty associated with background fields is characterized by the background error covariance matrix (***B***-matrix). The ***B-***matrix for temperature, specific humidity, and skin temperature is obtained from the NWPSAF 1D-Var package. The sensitivity to background error variance values for surface wind speed is estimated using collocated and concurrent RapidScat measurements, keeping the ***R-***matrix constant. Table 7 presents the average bias and standard deviation estimated from collocated and concurrent RapidScat measurements for different background error standard deviation values of wind speed. The wind speed BE variance is set to the square of the wind speed SD in the ***B-***matrix. The experiment was conducted separately again using only five channels (Channels 12-16) and seven channels (Channels 12-18) with brightness temperature bias correction. The average bias and standard deviations for the common collocations with RapidScat for ERA5 profiles and NWP SAF profiles are shown in Table 7, i.e., all numbers in this table are based on the same set of retrieved winds. A wind speed SD of 0.9 m/s provides the optimal balance between retrieved bias and SDD, resulting in the least overall deviation from RapidScat measurements. Additionally, using seven SSMIS channels further improves accuracy compared to using five channels. The average bias and SDD for the common collocations with ECMWF model winds for ERA5 profiles and NWP SAF profiles are shown in Table 8 for 1-9 October, 2014. Due to the large number of collocations with ECMWF model winds, 9 days of observations are included to obtain reliable statistics. As expected, we find that the average bias and SDD decrease with decreasing wind speed background error variance when compared to ECMWF model winds, as 1DVAR puts more weight on the prior ECMWF winds.

	Background profile: ERA5							
	No. of common collocations with RapidScat: 994,952							
	5 channels				7 channels			
Wind Speed BE SD (ms^{-1})	**1.4**	**1.1**	**0.9**	**0.7**	**1.4**	**1.1**	**0.9**	**0.7**
Average Bias (ms^{-1})	0.17	0.11	0.08	0.05	0.13	0.13	0.09	0.06
SDD (ms^{-1})	1.05	1.00	0.99	1.00	1.03	0.98	0.97	0.99
	Background profile: NWP SAF model profile							
	No. of common collocation with RapidScat: 1,089,659							
	5 channels				7 channels			
Wind Speed BE SD (ms^{-1})	**1.4**	**1.1**	**0.9**	**0.7**	**1.4**	**1.1**	**0.9**	**0.7**
Average Bias	0.31	0.24	0.19	0.15	0.55	0.45	0.39	0.33
SDD (ms^{-1})	1.16	1.14	1.13	1.13	1.20	1.16	1.15	1.14

Table 7: Average bias and SDD for collocated and concurrent RapidScat measurements at different wind speed background error (BE) variance, using five and seven SSMIS channels during October 2014 for ERA5 and NWP SAF prior model profiles.

	Background profile: ERA5							
	No. of common collocation with ECMWF: 8,114,650							
	5 channels				7 channels			
Wind Speed BE SD (ms^{-1})	**1.4**	**1.1**	**0.9**	**0.7**	**1.4**	**1.1**	**0.9**	**0.7**
Average Bias (ms^{-1})	0.18	0.12	0.08	0.05	0.13	0.13	0.09	0.06
SDD (ms^{-1})	0.73	0.52	0.38	0.25	0.76	0.54	0.40	0.26
	Background profile: NWP SAF model profile							
	No. of common collocation with ECMWF: 8,755,084							
	5 channels				7 channels			
Wind Speed BE SD (ms^{-1})	**1.4**	**1.1**	**0.9**	**0.7**	**1.4**	**1.1**	**0.9**	**0.7**
Average Bias (ms^{-1})	0.45	0.37	0.31	0.26	0.63	0.53	0.47	0.41
SDD (ms^{-1})	0.98	0.91	0.87	0.84	1.06	0.96	0.91	0.87

Table 8: Average Bias, SDD and no. of collocations with ECMWF wind speed at different wind speed background error SD, using five and seven SSMIS channels on 01-09 October 2014.

3.6. Validation

The retrieved wind speeds are validated using RapidScat data. The RapidScat instrument was in an inclined orbit of 51.6° and hence provides collocated and concurrent measurements with the polar orbiting SSMIS [15]. The spatial resolutions of RapidScat and SSMIS wind products are both 25 km, resulting in an effective minimum collocation distance of approximately 17.7 km (i.e., 25 km/√2). Figure 4(a) shows the number of collocations per grid point (~17.7km x17.7km) from 04 to 31 October 2014 and Figure 4 (b) shows the mean time difference between the collocated observations. For validation against RapidScat observations only the near surface wind speeds collocated within 17.7 km and 30 minutes are selected. Due to the large number of collocations one month of data is sufficient to validate SSMIS wind retrievals statistically. However, the validation could well depend on season, due to ancillary geophysical dependencies, like humidity or water content. Both scatterometers and radiometers are sensitive to the ocean surface roughness, which is related to the 10-m stress-equivalent wind for the scatterometer Normalized Radar Cross Section (NRCS) measurements hence NRCS and T_B measurements are insensitive to effects of air mass density and air mass stability, while the background winds used for SSMIS retrieval (simulated T_B) are only corrected through a mean bias correction, while both air mass stability and air mass density are transient and variable [16].

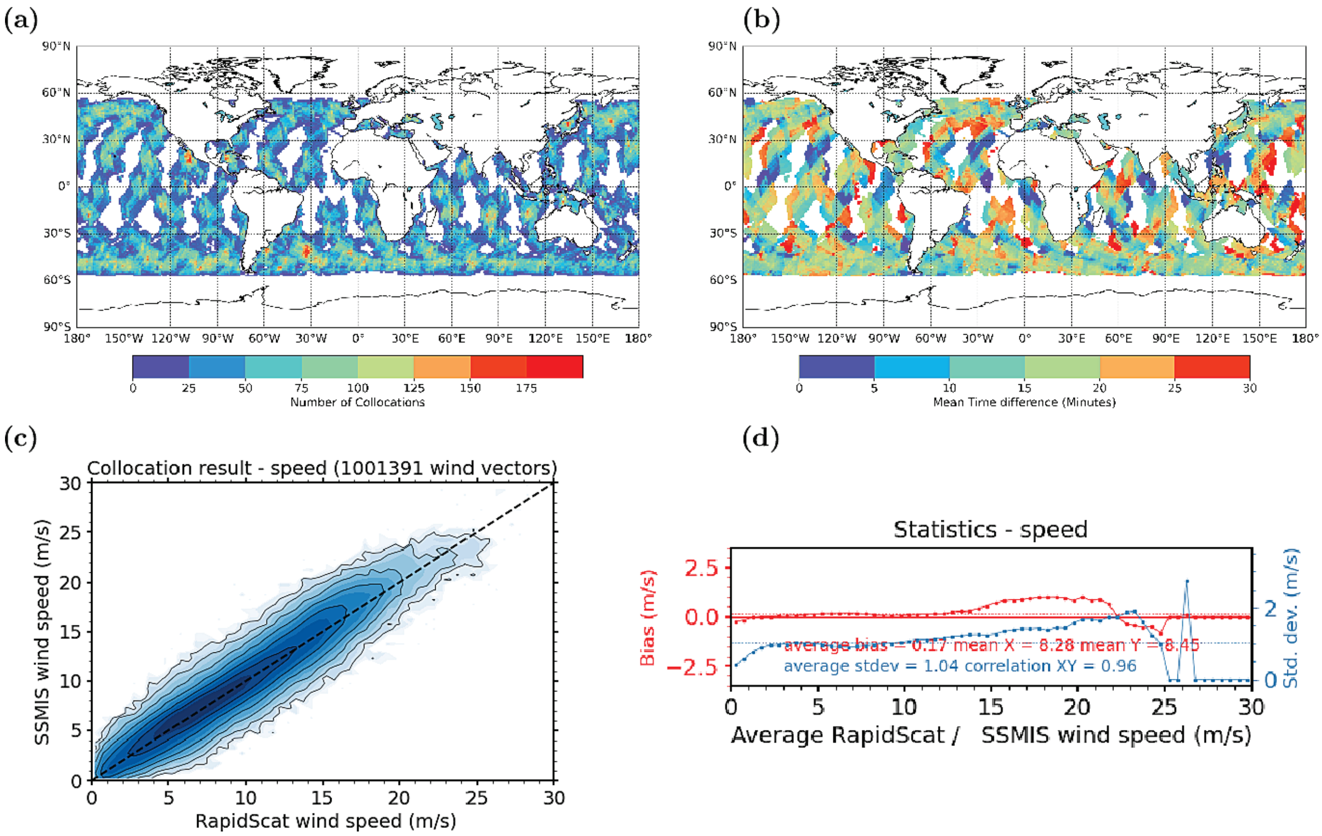

Figure 4 :(a) Number of SSMIS near-surface wind speed collocations with RapidScat during October 2014, and (b) the mean time difference between collocated observations. (c) Two-dimensional histogram of SSMIS wind speed (retrieved using 7 channels) versus RapidScat wind speed using ERA5 background profiles. (d) Average standard deviation (blue) and average bias (red) as a function of RapidScat wind speed during October 2014.

The Figure 4 (c) shows the two-dimensional histogram of SSMIS versus RapidScat wind speed for every 0.5 m/s bin, after quality control, for all orbits from 4 to 31 October 2014 using ERA5 background profiles. Since RapidScat winds are not assimilated in the ERA5 wind product, the dataset serves as an independent source for validating SSMIS wind retrievals. RapidScat wind speed collocated within 17.7 km (the swath grid cell spacing divided by √2) and concurrent within 30 minutes are used to validate SSMIS retrievals. The contours are in logarithmic scale. The wind speed background error variance for the retrievals is initially set to the square of the wind speed standard deviation of 1.4 m/s (the default value in NWPSAF 1D-Var). The average SDD between RapidScat and SSMIS wind speed is 1.04 m/s. Figure 4(d) shows the average SDD and bias as a function of average RapidScat and SSMIS wind speed. The comparison shows a strong agreement between SSMIS and RapidScat wind speed, with a very small bias (0.17 m/s) and a high correlation (0.96). For winds above 12 m/s SSMIS appears biased high generally by about 1 m/s.

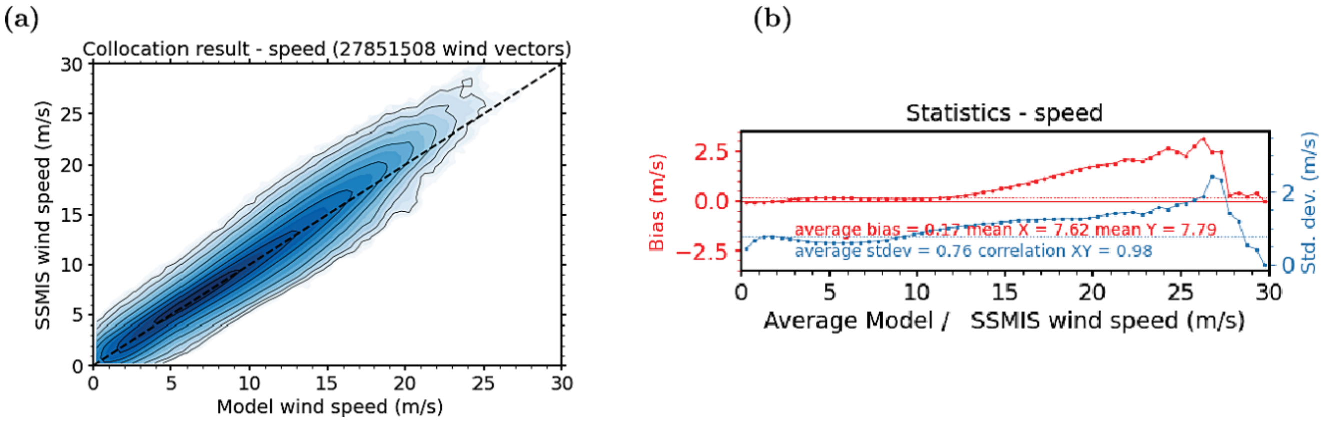

Figure 5: Two-dimensional histogram of SSMIS wind speed with ECMWF ERA5 stress-equivalent winds, (b) the average standard deviation (blue) and average bias (red) as a function of average SSMIS and ECMWF wind speed for October 2014.

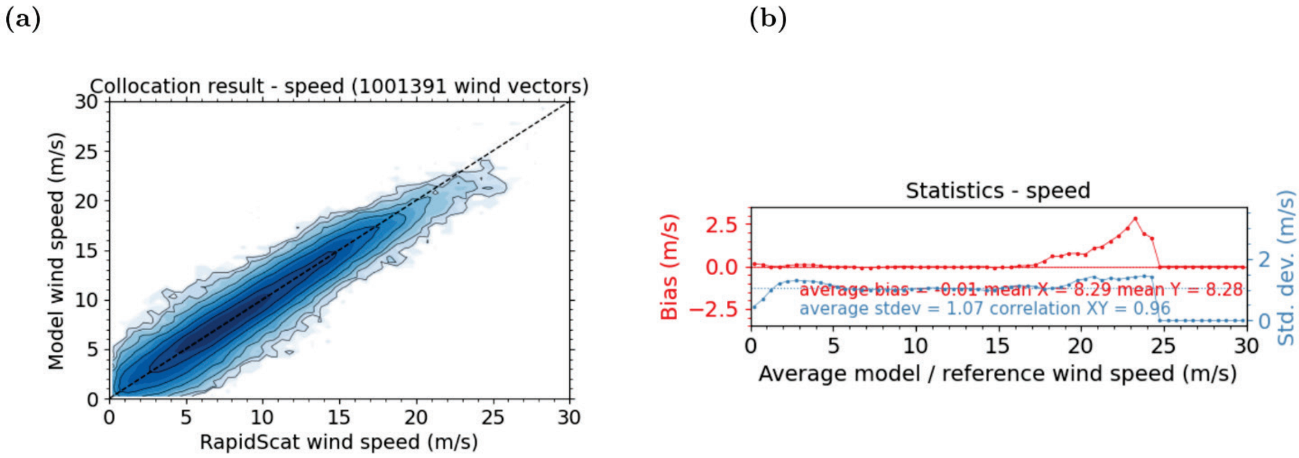

Figure 6: Two-dimensional histogram of RapidScat wind speed with ECMWF ERA5 stress-equivalent winds, (b) the average standard deviation (blue) and average bias (red) as a function of average SSMIS and ECMWF wind speed for October 2014.

Figure 5 shows the dependent validation of retrieved wind speeds (using ERA5 background profiles) against ECMWF model wind speeds. The SSMIS wind speed exhibits an average bias of 0.17 m/s with a relatively low average standard deviation of 0.76 m/s. The bias remains near zero for most wind speeds but substantially increases at higher wind speeds. In fact, the 1D-Var cost function at high wind speed appears dominated by the wind speed bias, which will result in a large difference between measured and simulated T_B. As Bayesian retrieval should be unbiased, a T_B dependent bias correction appears necessary for optimal 1D-Var retrieval. The SDD remains consistently low, and the high correlation (0.98) indicates strong agreement between SSMIS and ECMWF model winds, as expected. Figure 6 shows the comparison of collocated and concurrent ERA5 winds speed with RapidScat during October 2014. The average bias is 0.01 m/s with an average SDD of 1.07. The bias tends to increase at higher wind speeds for ERA5 when compared to RapidScat (in Figure 6(b)), however the bias is noticeably reduced at higher wind speeds in the case of SSMIS relative to RapidScat, as illustrated Figure 4(d). Similarly, the SDD is 1.04 m/s for SSMIS wind speeds, while it increases to 1.07 m/s for ERA5 wind speeds when compared to RapidScat winds.

4. Wind Retrievals: Spatial Distribution

4.1. Near-surface wind retrieval for all-sky

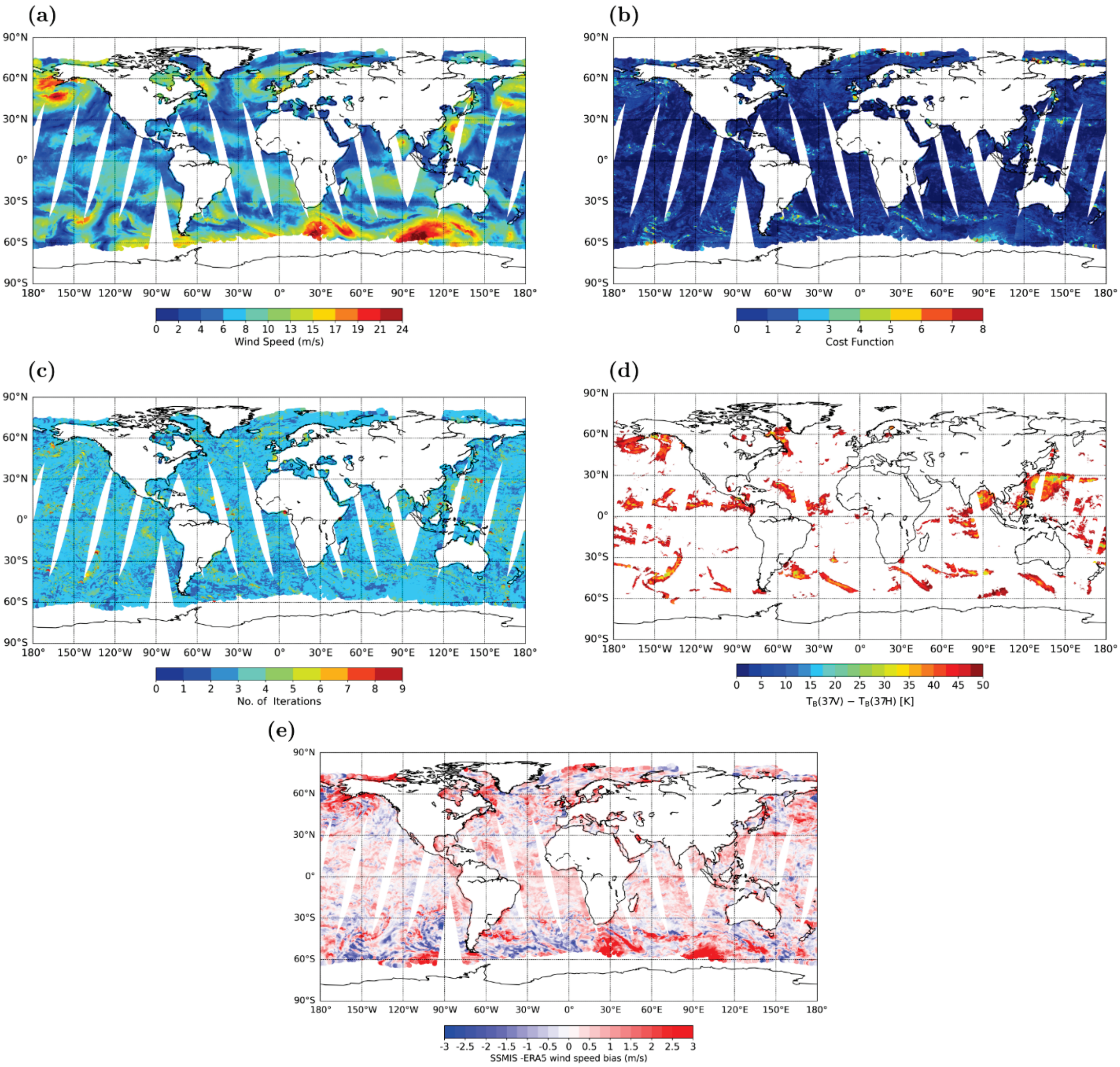

Figure 7: Surface wind speed retrievals from SSMIS (b) the cost function for each pixel (c) the number of iterations required to attain convergence for all-sky conditions for ERA5 profiles, (d) rainy pixels identified from SSMIS brightness temperature, (e) the bias between SSMIS wind speed and ERA5 model wind speed for seven consecutive orbits on 09 October 2014.

The results presented in the following section include wind speed retrievals using ERA5 background profiles for 9 October 2014, covering seven consecutive ascending and descending orbits. The current method enables wind retrieval under all-sky conditions. Figure 7 (a) illustrates the near-surface wind speed retrieved from SSMIS T_B data using this approach. To identify rainy cases, a rain flag based on SSMIS brightness temperature is applied, following [17]. Pixels are classified as rain-contaminated if $T_B(37V)$ - $T_B(37H)$ < 50K or $T_B(19H)$ > 165K. Figure 7(b) presents the cost function values for successful retrievals, with an average value below 1.0 for clear-sky cases within a single satellite swath. Similarly, Figure 7(c) depicts the number of iterations required for convergence in successful retrievals. On average, convergence is achieved after three iterations for all-sky conditions in each satellite swath, with an average cost function value below 1.0 per swath. The rain contaminated pixels are shown in Figure 7(d). For rainy pixels, the number of iterations required for convergence is slightly higher, ranging from 5 to 7. Currently, the criteria based on the threshold for the cost function result in a rejection of wind retrievals varying between 9-15% for each SSMIS swath. Applying the rain flag along with the above criteria results in a further rejection of 6% of the wind retrievals for the seven consecutive orbits shown in Figure 7 (a). Figure 7(e) illustrates the difference between SSMIS wind speed and ERA5 wind speed. The wind speed bias is pronounced over regions with high wind speeds, particularly near 60° latitude in both hemispheres and rain contaminated pixels. Even though RTTOV-SCATT simulates radiances under all-sky conditions, wind retrievals for rain-contaminated pixels and regions of high wind speed require further investigation.

4.2. Comparison of wind retrieval under all sky and clear sky conditions

Table 9 presents the comparison of SSMIS wind retrievals with both RapidScat wind speeds and ECMWF model wind speeds under all-sky conditions and clear sky cases. The rain flag applied based on SSMIS brightness temperature as shown in Figure 7 (d). As expected, the average bias and standard deviation improved in the clear sky cases. However, applying the rain flag results in a further rejection of 11-13% of wind retrievals in October 2014. The rain-flagged winds are then compared to collocated RapidScat measurements. The average standard deviation of rain flagged pixels with RapidScat wind speed is 1.44 m/s, with an average bias of 0.28 m/s. Note that in rainy scenes, the ECMWF winds usually also have larger errors, since the model usually doesn't capture the winds from small scale downdrafts associated with heavy rain. Also, the RapidScat instrument, operating in Ku-band, is sensitive to rain and despite thorough quality control, winds may have larger errors in case of rain.

	All sky condition		Clear sky condition	
	RapidScat	ECMWF	RapidScat	ECMWF
Avg. Bias (ms^{-1})	0.17	0.17	0.15	0.17
SDD (ms^{-1})	1.04	0.76	0.96	0.72
No of collocations	1,001,391	27,851,508	866,885	24,475,297

Table 9: Average bias, SDD, and number of collocations of SSMIS wind retrievals for ERA5 background profiles with RapidScat and ECMWF model winds for all-sky and clear sky conditions during October 2014.

5. Conclusions

The 1D-Var retrieval algorithm was employed to retrieve near-surface wind speed from SSMIS brightness temperature data. The RTTOV forward model, along with RTTOV-SCATT (scattering module), was used to compute radiance at SSMIS frequencies at the top of the atmosphere under all-sky conditions. For background profiles, both the NWP SAF model profile database and ERA5 forecast data were used. The ERA5 forecast data provided better retrievals than the selected NWP SAF model profiles, in terms of wind speed bias and standard deviation with respect to independent RapidScat winds. Independent and intercalibrated wind vectors from RapidScat measurements are used to optimize the 1D-Var retrievals. The algorithm was implemented as a preparation for processing of the EPS-SG MWI data that will be on the same platform as SCA, the EPS-SG scatterometer. Experimental runs were conducted separately using (i) five channels (Channels 12-16) and (ii) seven channels (Channels 12-18) for different wind speed background error values. The optimal value of wind speed background error was estimated using collocated and concurrent RapidScat winds. The wind retrievals using ERA5 as the background profile and with seven SSMIS channels provided more accurate wind retrievals when compared with collocated and concurrent RapidScat measurements.

To improve the accuracy of wind retrievals under all-sky conditions, the following areas require further investigations:

- RTTOV-SCATT successfully simulates brightness temperatures under all-sky conditions, but T_B-dependent biases remains. Currently the systematic brightness temperature biases are corrected for each SSMIS channel. To ensure unbiased Bayesian retrieval, a more refined T_B-dependent bias correction may be required for optimal 1D-Var retrieval for rain contaminated pixels.
- Rain-contaminated pixels show elevated cost function values and require more iterations during wind retrieval, indicating a need for further characterization with respect to retrieval error and QC.
- The current cost function threshold (8.0) should be validated and potentially refined using collocated scatterometer measurements to improve quality control, especially under rainy conditions.
- The B-matrix is currently taken from NWPSAF 1D-Var, are there better alternatives?
- ERA5 profiles yield better results than NWPSAF profiles, however, the current use of 137 vertical levels and full horizontal resolution may be excessive. The resolution and granularity has to be determined since the 1D-Var system uses only 43 vertical levels.

6. References

[1] Vogelzang, J. and A. Stoffelen, On the Accuracy and Consistency of Quintuple Collocation Analysis of In Situ, Scatterometer, and NWP Winds, *Remote Sens.*, 2022, 14, 18, 4552, doi:10.3390/rs14184552

[2] Ni, W., A. Stoffelen, K. Ren, X. Yang and J. Vogelzang, SAR and ASCAT Tropical Cyclone Wind Speed Reconciliation, *Remote Sens.,* 2022, 14, 5535, doi:10.3390/rs14215535

[3] Ricciardulli L. and A. Manaster, Intercalibration of ASCAT Scatterometer Winds from MetOp-A, -B, and -C, for a Stable Climate Data Record, *Remote Sens.*, 2021, 13, 18, 3678, doi:10.3390/rs13183678

[4] Vogelzang, J. and A. Stoffelen, Improvements in Ku-band scatterometer wind ambiguity removal using ASCAT-based empirical background error correlations, Q J R Meteorol Soc. 2018; 144, 2245–2259, doi:10.1002/qj.3349

[5] Stoffelen, A., A. Mouche, F. Polverari, G.-J. van Zadelhoff, J. Sapp, M. Portabella, P. Chang, W. Lin and Z. Jelenak, C-band High and Extreme-Force Speeds (CHEFS), EUMETSAT/KNMI, 2020

[6] Belmonte Rivas, M., A. Stoffelen, J. Verspeek, A. Verhoef, X. Neyt and C. Anderson, Cone Metrics: A New Tool for the Intercomparison of Scatterometer Records, *IEEE Journal of Selected Topics in Applied Earth O*, 2017, 10, 5, 2195-2204, doi:10.1109/JSTARS.2017.2647842

[7] EUMETSAT. n.d. Metop-SG MWI L1B Data Guide, [Online]. Available: https://user.eumetsat.int/resources/user-guides/metop-sg-mwi-l1b-data-guide

[8] Graw, K., J. Kinzel, M. Schröder, K. Fennig and A. Andersson, Validation Report SSM/I and SSMIS products HOAPS version 4.0, CM SAF, 2017

[9] Rodgers, C.D., Inverse Methods for Atmospheric Sounding, World Scientific, 2000, doi:10.1142/3171

[10] Geer, A. J., P. Bauer, K. Lonitz, V. Barlakas, P. Eriksson, J. Mendrok, A. Doherty, J. Hocking and P. Chambon, Bulk hydrometeor optical properties for microwave and sub-millimetre radiative transfer in RTTOV-SCATT v13.0, *Geosci. Model Dev.*, 14, 7497–7526, 2021, doi:10.5194/gmd-14-7497-2021

[11] Kilic, L., C. Prigent, C. Jimenez, E. Turner, J. Hocking, S. English et al., Development of the SURface Fast Emissivity Model for Ocean (SURFEM-Ocean) based on the PARMIO radiative transfer model, *Earth and Space Science*, 10, e2022EA002785, 2023 doi:10.1029/2022EA002785

[12] Eresmaa, R. and A. McNally, Diverse profile datasets from the ECMWF 137-level short-range forecasts, NWP SAF, 2014

[13] Stoffelen, A., J. Vogelzang and G.J. Marseille, High-resolution wind data assimilation guide, version 1.3, SAF/OSI/CDOP3/KNMI/SCI/GUI/388, EUMETSAT, 2020

[14] Hwang, P. A., Foam and Roughness Effects on Passive Microwave Remote Sensing of the Ocean, *IEEE Transactions on Geoscience and Remote Sensing*, 50, 8, 2978-2985, 2012, doi: 10.1109/TGRS.2011.2177666

[15] OSI SAF Winds Team, Product User Manual (PUM) for the Ku-band wind data records, SAF/OSI/CDOP3/KNMI/TEC/MA/414, EUMETSAT, 2023

[16] De Kloe, J., A. Stoffelen and A. Verhoef, Improved Use of Scatterometer Measurements by Using Stress-Equivalent Reference Winds, *IEEE Journal of Selected Topics in Applied Earth O*, 2017, 10, 5, 2340-2347, doi:10.1109/JSTARS.2017.2685242

[17] Connor, L. N. and P. S. Chang, Ocean surface wind retrievals using the TRMM microwave imager, IEEE Transactions on Geoscience and Remote Sensing, 38, 4, 2009-2016, 2000, doi: 10.1109/36.851782

[18] Hocking, J., RTTOV v14 Users' Guide, NWPSAF-MO-UD-055, EUMETSAT, 2025

7. Abbreviations and acronyms

1DVAR	1-dimensional Variational Retrieval
B-matrix	Background Error Covariance Matrix
BE	Background Error
CM SAF	Climate Monitoring Satellite Application Facility
EPS-SG	EUMETSAT Polar System – Second Generation
EUMETSAT	European Organisation for the Exploitation of Meteorological Satellites
HOAPS	Hamburg Ocean Atmosphere Parameters and Fluxes
KNMI	Royal Netherlands Meteorological Institute
MWI	Microwave Imager
NASA	National Aeronautics and Space Administration
NWP	Numerical Weather Prediction
OSI SAF	Ocean and Sea Ice Satellite Application Facility
QC	Quality Control
R-matrix	Observational Error Covariance Matrix
RapidScat	SeaWinds-like scatterometer on-board the International Space Station
RTTOV	Radiative Transfer for TOVS
RTTOV-SCATT	RTTOV-Scattering module
SAF	Satellite Application Facility
SDD	Standard Deviation Difference
SSMI	Special Sensor Microwave Imager
SSMI/S	Special Sensor Microwave Imager Sounder
SST	Sea Surface Temperature
T_B	Brightness Temperature